Control Systems Principles Applied to Speckle Filtering and to the Retrieval of Soil Physical Parameters through ERS and RADARSAT SAR Data Fusion

Edmond NEZRY, Francis ZAGOLSKI, Francis YAKAM-SIMEN, Iwan SUPIT

PRIVATEERS N.V. Private Experts in Remote Sensing,
De Weaver Drive 42, Philipsburg, Sint Maarten, Netherlands Antilles,
c/o 228 Gillespie street, Sherbrooke (Qc), CANADA J1H-4X3.

Phone/Fax: (+39) 332-781494 / (+1) 819-569-7632
E-mail: edmond.nezry@iol.it / zagolski@interlinx.qc.ca
Internet Homepage: http://www.treemail.nl/privateers

ABSTRACT

Two new Bayesian Maximum A Posteriori (MAP) vector speckle filters are developed for multi-channel detected Synthetic Aperture Radar (SAR) images. These filters incorporate statistical descriptions of the scene and of the speckle in multi-channel SAR images. These models account for the scene and system effects which result in the presence of a certain amount of correlation between the different channels.
In order to account for the effects due to the spatial correlation of both the speckle and the scene in SAR images, estimators originating from the local autocorrelation functions (ACF) are incorporated to these filters, to refine the evaluation of the non-stationary first order local statistics, to improve the restoration of the scene textural properties, and to preserve the useful spatial resolution in the speckle filtered image.
Since the new established Bayesian speckle filters present the structure of control systems, their application is the first processing step of application-oriented control systems designed to exploit the synergy of SAR sensors. We present here such a control system, designed to retrieve soil roughness and soil moisture through Bayesian ERS / RADARSAT data fusion.
Results obtained on a couple of ERS PRI and RADARSAT Standard Beam SAR images show that the new speckle filters present convincing performances for speckle reduction, for texture preservation and for small scene objects detection. The retrieval of soil roughness and soil moisture through Bayesian data fusion of ERS and RADARSAT data provides also valuable results for the monitoring of agriculture and environment.

1. INTRODUCTION

Although numerous work with regard to multi-channel speckle filtering in SAR images has already being done in the past, some important issues of interest remain still open. Among them, the introduction of A Priori knowledge or A Priori guess which implies the use of Bayesian methods in the processing of multi-SAR's images, multi-date SAR images or SAR and Optical images. So far, the case of multi-channel detected SAR images had not yet been studied with this approach.
Among the Bayesian methods, the Maximum A Posteriori (MAP) filtering method has already proved to be particularly suited for the restoration of both the radar reflectivity and the textural properties of the imaged scene in the case of mono-channel detected SAR images [1].
In the case of multi-channel detected SAR images, let define the vector quantities of interest: I is the speckled intensity vector available in the actual SAR data; R is the radar reflectivity vector which is the quantity we will to restore. The MAP filtering method bases on the famous Bayes' theorem (1828):

$$P(R/I) = P(I/R) \,.\, P(R) / P(I) \qquad (1)$$

$P(I/R)$ is the joint probability density function (pdf) of the speckle. With regard to each individual detected SAR image, $P(I_i/R_i)$ is well known to be a Gamma distribution for multilook intensity images. $P(R)$ is the joint pdf of the radar reflectivity. This last pdf is introduced as statistical A Priori information in the restoration process. To describe the first order statistical properties of natural scenes, it has already been shown that a Gamma distribution is suitable as a choice for $P(R_i)$.

For multi-channel detected SAR images, MAP Filtering is a vector filtering method. For any channel i, the posterior probability is maximum if the following condition is verified:

$$\partial[\mathrm{Ln}(P(I/R))]/\partial R_i + \partial[\mathrm{Ln}(P(R))]/\partial R_i = 0 \quad \text{for} \quad \hat{R}_i = R_{i\,MAP}, \text{ the MAP estimation of } R_i \tag{2}$$

The first term of Eq. 2, (Maximum Likelihood term) accounts for the effects of the whole imaging system. The second term, (Maximum A Priori term) represents the prior statistical knowledge with regard to the imaged scene.
In the Bayesian approach, probabilities are used to describe incomplete information rather than randomness. As it should be noted in Eq. 2, in the Bayesian inference process, induction is influenced by the prior expectations allowed by the prior knowledge of P(*R*) [2]. In addition, the non-linear system and scene effects are taken into account by the restoration process. Therefore the MAP speckle filtering can be considered as a controlled restoration of R, where A Priori knowledge controls the inference restoration process and allows an accurate estimation of the radar backscattering coefficients σ°_i.
At this point, additional Bayesian processes can be designed to retrieve important geophysical parameters, in a cascade of control processes.

2. MULTI-CHANNEL SCENE MODEL

To describe the first order statistical properties of a natural scene as viewed at the spatial resolution of the spaceborne remote sensing sensors, it has been established that a Gamma pdf would be the most suitable representation. However, to describe the first order statistical properties of a natural scene as viewed by diverse SAR sensors (different physical features of the scene), or at different dates (scene evolution with time), there is no analytic multivariate Gamma pdf available.
Therefore, we will use in the following a multivariate Gaussian pdf as analytic multi-channel scene statistical model:

$$P(R) = [(2\pi)^N\,|\mathrm{Cov}_R|]^{-1/2} \,.\, \exp[\, -\, {}^t(R-\langle R\rangle).\mathrm{Cov}_R^{-1}.(R-\langle R\rangle)] \tag{3}$$

where Cov_R is the covariance matrix of the imaged scene.
This statistical model is convenient to preserve the mathematical tractability of the problem. In addition, the Gaussian model is the most commonly used to describe the statistical properties of natural scenes.

3. SPECKLE UNCORRELATED BETWEEN CHANNELS: THE GAMMA-GAUSSIAN MAP FILTER

In this section, we will consider the case of very different SAR sensors (very different wavelengths, for instance). In this case, it is justified to consider that the speckle is independent between the N image channels. Under this assumption, P(*I*/*R*) can be modelled as a set of N independent Gamma distributions $P(I_i/R_i)$:

$$P(I_i/R_i) = (L_i/R_i)^{L_i} / \Gamma(L_i) \,.\, \exp(-L_i\, I_i/R_i) \,.\, I_i^{(L_i-1)} \tag{4}$$

where the L_i parameters are the Equivalent Numbers of Looks (ENL) of the individual SAR images.

Under this assumption, our first MAP filtering algorithm for multi-channel detected SAR images comes down to the resolution of a set of N scalar equations, with N independent speckle models and a coupled scene model (since the physical properties of the scene do contribute, but not in the same amount, to the formation of the images provided by the different sensors). The set of equations describing the ***Gamma-Gaussian MAP filter for multi-channel detected SAR images*** is as follows [3]:

$$\begin{aligned} L_i\,(I_i/R_i^2 - 1/R_i) - {}^t(1_i).\mathrm{Cov}_R^{-1}.(R-\langle R\rangle) - {}^t(R-\langle R\rangle).\mathrm{Cov}_R^{-1}.(1_i) - 1/2\ \mathrm{Tr}[\mathrm{Cov}_R^{-1}.\partial\mathrm{Cov}_R/\partial R_i] \\ + {}^t(R-\langle R\rangle).\mathrm{Cov}_R^{-1}.\partial\mathrm{Cov}_R/\partial R_i\,.\mathrm{Cov}_R^{-1}.(R-\langle R\rangle) = 0 \end{aligned} \tag{5}$$

where (1_i) is a vector where all components, but the i^{th}, are equal to zero. The set of Eqs. 5 are solved numerically.

Replacing the speckle noise model by an optical noise (or film grain noise, or any other appropriate noise model) in some of the N image channels, this filter adapts easily to the case of multi-channel optical and SAR images. Thus, the introduction of coupling between the scene statistical representations is already a data fusion process.

4. SPECKLE CORRELATED BETWEEN CHANNELS: THE GAUSSIAN-GAUSSIAN MAP FILTER

In the case of multi-date images acquired on repeat-pass by the same SAR sensor (a common interesting case, regarding ERS, RADARSAT, etc.), or of a set of SAR images acquired by diverse SAR's with some similar properties (similar orbit, track, frequency and spatial resolution, with difference in polarisation configuration only, or small differences in incidence angle, for example), the development of a second speckle filtering algorithm can be considered. In this cases, the correlation of the speckle should be taken into account to deal optimally with system effects on the series of SAR images.
If the speckle correlation between image channels is taken into consideration, the joint pdf of the speckle P(I/R) should theoretically be a multivariate Gamma pdf. Nevertheless, since there is no analytic multivariate Gamma pdf available, another reasonable choice for P(I/R) should be done for the sake of mathematical tractability.
To solve this problem, we will adopt Lee's assumption: Lee [4] has shown that, in the case of multilook SAR images (more than 3 looks), the pdf of the speckle can be reasonably approximated by a Gaussian distribution. Therefore, for convenience, P(I/R) is approximated by a Gaussian multivariate distribution in the case of multilook SAR images:

$$P(I/R) = [(2\pi)^N |Cov_S|]^{-1/2} . \exp[- {}^t(I-R).Cov_S^{-1}.(I-R)] \quad (6)$$

where Cov_S is the covariance matrix of the speckle.

Under this assumption, our second MAP filtering algorithm, for multi-channel detected multilook SAR images, comes down to the resolution of a set of N scalar equations, with coupled speckle and scene models. The set of equations describing the ***Gaussian-Gaussian MAP filter for multi-channel detected multilook SAR images*** is as follows [3]:

$$ {}^t(1_i).Cov_S^{-1}.(I-R) + {}^t(I-R).Cov_S^{-1}.(1_i) - 1/2\ Tr[Cov_R^{-1}.\partial Cov_R/\partial R_i]+ {}^t(R-<R>).Cov_R^{-1}.\partial Cov_R/\partial R_i .Cov_R^{-1}.(R-<R>)$$
$$ - {}^t(1_i).Cov_R^{-1}.(R-<R>) - {}^t(R-<R>).Cov_R^{-1}.(1_i) = 0 \quad (7)$$

The set of Eqs. 7 are again solved numerically.

5. ADVANTAGES OF THESE FILTERS. MAP FILTERING AND CONTROL SYSTEMS

A number of advantages and improvements these filters offer are listed in this section. Most of these advantages arise from the use of the covariance matrices of the speckle and of the imaged scene (*i.e.* from the use of coupled models) in a Bayesian reconstruction of the radar reflectivity.

5.1. Non linear image restoration:

A number of different techniques have already been proposed in the past for multi- SAR image filtering. Generally, the only point of similarity between these techniques is their common use of models that do not account for the non-linearity's of SARA image formation. These non-linearity's are taken into account in the MAP inference process.

5.2. Imaging system's effects and preservation of high-resolution:

In a series of SAR (but not only...) images, the resolution cells never overlap perfectly between the different individual images. The covariance matrix of the speckle Cov_S contains the information about these overlaps, and the filtering process accounts for

these overlaps in order to preserve, and even improve the spatial resolution in the filtered SAR images, thus allowing us to restore the thinnest scene structures.
In addition, the simultaneous attempt to detect images structures and targets in all the SAR image channels, allows to improve the probability to detect such structures. As it will shown in the application examples, such an improvement is already very substantial using only two SAR images.

5.3. Potential for change detection:

The covariance matrix of the scene Cov_R contains the information about the temporal evolution of the imaged area:
In the case of a multi-date time series acquired by the same SAR sensor on repeat-pass mode, the covariance matrix of the scene enables the detection of changes in scene physical properties (scene temporal evolution). In the case of a series of SAR images acquired by (not too...) different SAR's, the covariance matrix of the scene enables the detection of more aspects of the scene, as it is viewed by more SAR sensors.

5.4. Analogy with control (or communication) systems:

Let consider the mathematical form of the set of Equations 8 and 13. Their formulation presents a striking analogy to that of a control system. Both Eqs. (5) and (7) can be rewritten as Riccati's algebraic (matricial) equations:

$$- A X - X {}^{t}A - Q + X {}^{t}C P^{-1} C X = 0 \quad (8)$$

Equation (4) represents the optimal state controlled reconstruction at constant gain of linear invariant processes (*R* and textures of the channels) perturbed by white noises (speckle, pixel spatial mismatch between channels). The scene A Priori model acts as a command, and the covariance matrices act as multipoles or controls. It is also noticeable that the MAP elaboration of information generates automatically the feedback processes which enable to control the filtering process itself.
In addition, Riccati's theorem stipulates the existence of a unique positive definite solution for Eq. (8). Therefore, this property holds also for the MAP equations (5) and (7).

6. IMAGE PROCESSING ASPECTS: IMPLEMENTATION ALGORITHMS

The main classic assumptions behind the theory used to design these filters are that:
- A Non-stationary Mean Non-stationary Variance (NMNV) first order statistical model is assumed to justify local treatment (processing window) using local statistics. Therefore, second order statistical spatial properties (spatial correlation) of all the individual SAR images must also be considered to include both scene texture and resolution/sampling related properties, for an optimal restoration of the radar reflectivity.
- Scene ergodicity and stationarity are assumed. Compliance with this hypothesis requires the preliminary detection and identification of the structural elements of the scene.

6.1 Detection of scene structures using the Ratio of Amplitudes (RoA) detectors:

The first possible implementation algorithm including scene structures detection uses the RoA detectors for edges, linear features, or point targets and strong scatterers [5,1]. In this algorithm, structure detection is performed in terms of probability of detection and probability of false alarm (Pfa), using templates of various sizes and shapes within the processing window.
Detection is successfully performed and this algorithm is very efficient when the spatial correlation of the speckle is low between pixels. However, the performance of the RoA detectors is substantially degraded when the spatial correlation of speckle samples becomes significant. As shown in [6], spatial speckle correlation results in an increasing detection of non-existing structures, *i.e.* in the increase of the Pfa. In addition, the spatial speckle correlation also decreases the probability of detection, as also shown in [6]. The combination of these two effects cause artefacts in the filtered image (visual "crumbled paper" effect), and reduces the performance of further automatic image processing.

6.2 Detection of scene structures using two-points statistics:

Speckle can present strong spatial correlation properties (*e.g.* ERS PRI, RADARSAT Std. Beam) between pixels, a situation for which the detection algorithm based on the RoA detectors was not designed to cope with. In addition, using the NMNV scene

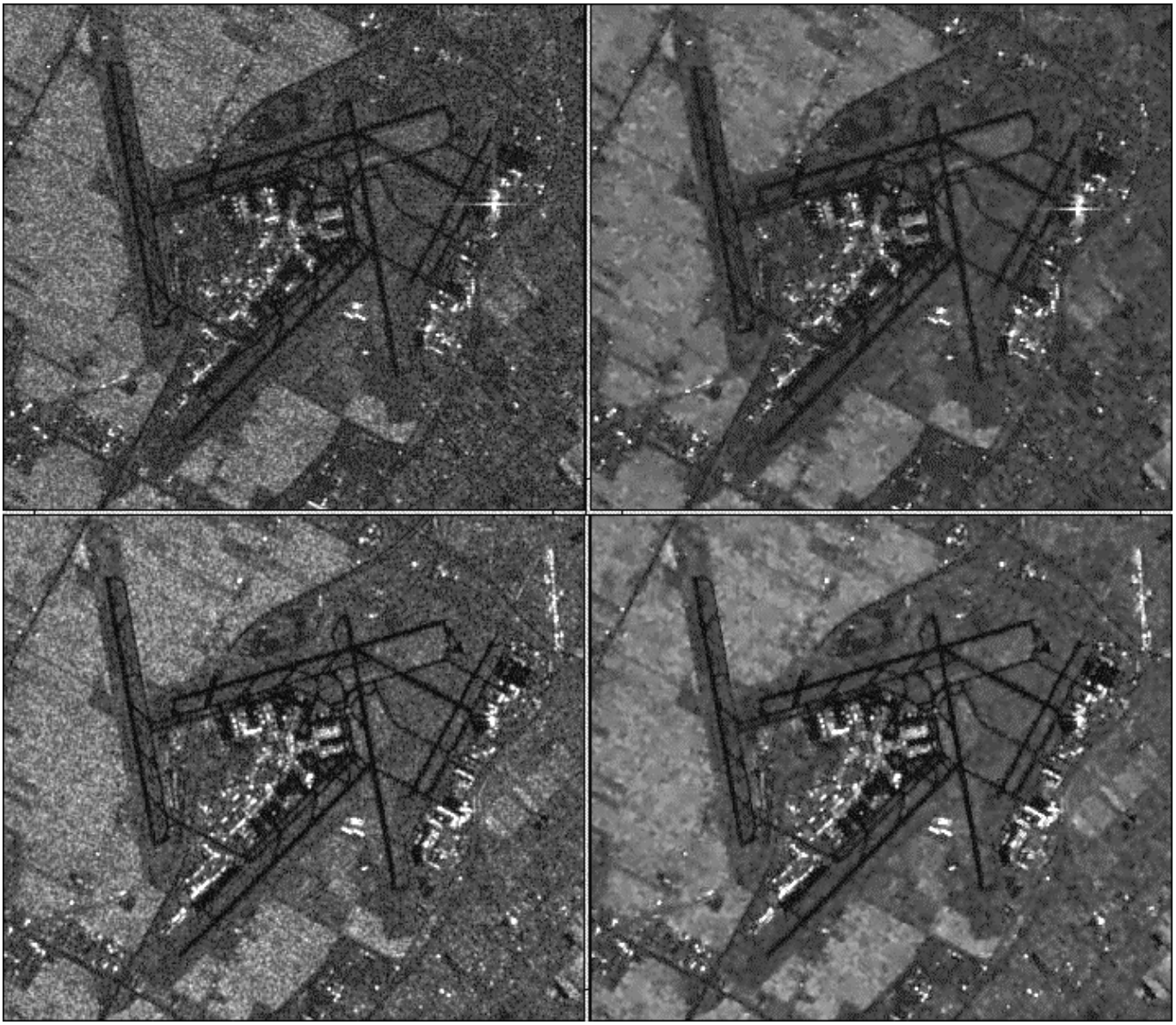

Figure 1: Upper images: ERS-1 PRI image (© ESA/Eurimage 1996) and its filtered version. Bottom images: RADARSAT Std Beam S1 image (© RADARSAT International 1996) and its filtered version (Gaussian-Gaussian MAP filter for multi-channel detected multilook SAR images).

model, one should consider that the estimation of the local reflectivity at the pixel under consideration needs to be corrected for the effects of tonal variations within the processing window.
To correct these drawbacks, locally estimated two-points statistics have been introduced in [6] to perform structure detection as

well as to refine the computation of the local NMNV first order statistics. This detection algorithm is inspired from the concept of "texture fields" [7]. This concept, based on the analysis of second order statistical properties, generalises image processing concepts such as filtering and detection, which are usually considered as distinct. It enables to perform simultaneously structure detection and image filtering.
Regarding speckle filtering, the local mean radar reflectivity estimation takes then into account the textural properties of the imaged scene (spatial variability of R between resolution cells, directionality) and the spatial correlation properties of the speckle. Introducing the estimates for the non-stationary local statistics into the scalar equation of a single-point filter improves the restoration of natural R fluctuations (texture) in the filtered SAR image, as it has already been shown in [6].
In addition, using this technique, the detection of even thin or low-contrast structures becomes implicit. Consequently, a specific structure detection associated to the filter is no longer needed, and the overall processing is greatly simplified. The major advantage is that there is no geometrisation of the scene structural elements, as it may happen using the templates-based RoA detectors [1]. The neighbourhood on which the NMNV local statistics are estimated is delimited by the two-points statistics in all possible orientations. The only limitation to the potential extension of this neighbourhood is the spatial extent of the available autocorrelation function of the speckle.
Incidentally, the estimation of the RADARSAT speckle acf (*i.e.* the RADARSAT point spread function) lead to an estimation of the spatial resolution achieved on Std. Beam S1 4-look images. The estimated spatial resolutions were about 17m in range and 18m in azimuth.

7. APPLICATION TO AN ERS PRI / RADARSAT STD. BEAM SAR IMAGES SET

Our new filtering technique are evaluated in the case of multi-sensor SAR images, on a couple of RADARSAT Std. Beam (C-HH, 4-look, resolution: 17x18m) and ERS PRI (C-VV, 3-look, resolution: 22x25m) SAR images. Both images were acquired on descending passes within 4 hours on 13 Feb. 1996, so the imaged scene experienced very little changes. Fig. 1 (left column) shows a detail of the RADARSAT (up) and ERS (bottom) images, around Amsterdam's airport (the Netherlands).
The RADARSAT and ERS SAR's operate at the same frequency, from a very similar orbit (similar altitude and inclination angle). The angles of incidence are also very similar (very close to 23° at the frame's center for both images). Therefore, image superimposition is possible without geometrical corrections on wide areas.
The two sensors differ only in polarisation configuration, so that they are sensitive to similar physical properties of extended land areas, even if these properties do not contribute in the same amount to the backscattered signal. However, their different sensitivity to structural scene elements is of major interest for the identification of these particular targets. In this context, it is appropriate to use the new Gaussian-Gaussian MAP filter for multi-channel detected multilook SAR images such a way that the structure information detected in one of the images is also exploited to filter the second one.
The filtered images are shown in Fig. 1 (right images). Thin details such as roads, runways, airport terminals, planes, point targets in the built-up areas, are very well denoised and preserved, as it is also the case for field edges. On the other hand, speckle noise is strongly filtered within the surrounding homogeneous agricultural fields (ENL=120 after filtering: for RADARSAT, ENL=100 for ERS). For both images, the filtered images were found superior in quality to the images filtered using the mono-channel Gamma-Gamma MAP filter [1] using the same structure detection algorithm [6].

8. RETRIEVAL OF SOIL ROUGHNESS AND SOIL MOISTURE FROM ERS/RADARSAT DATA FUSION

Haddad & Dubois [8] have developed a Bayesian estimation method of soil roughness and soil moisture. Although their method present some built-in limitations (the imaginary part of the dielectric constant ε is not taken into account, no dependence on the surface correlation, *cf.* [9]), it is based on the same principle as our new filtering method and present common theoretical advantages.
Since our data are accurately filtered and calibrated, instead of the model presented in [8], we can now use directly the soil backscattering empirical model of Dubois *et al.* [10]:

$$\sigma^{\circ}_{HH} = m = M_1(\theta,\lambda) \,.\, f(\varepsilon,h) \qquad (9)$$

$$\sigma^{\circ}_{VV} = n = M_2(\theta,\lambda) \,.\, g(\varepsilon,h)$$

where θ is the wave incidence angle, λ is the radar wavelength, ε is the soil dielectric constant, and h is the r.m.s. height (soil roughness). Using Bayes' theorem, the unnormalised version of the conditional joint probability of (ε,h) verifies [8]:

$$P(\varepsilon,h|m,n) = P(\varepsilon,h) \,/\, [\, f(\varepsilon,h).g(\varepsilon,h)\,] \,.\, P(M_1, M_2) \qquad (10)$$

The optimum unbiased estimator for $X \in \{\varepsilon,h\}$ that has minimum variance is the conditional mean [8]:

$$\hat{X} = \int X \,.\, P(\varepsilon,h|m,n)\, d\varepsilon.\, dh \qquad (11)$$

Finally, the dielectric constant is converted to volumetric soil moisture through a set of empirical curves [11].

With our data accurately filtered and calibrated, the nature of the randomness present in (m,n) can only be due to relief. Since our Netherlands area present negligible relief, $P(M_1, M_2)$, which depend primarily on the SAR frequencies and on the local incidence angles is reasonably assumed a Dirac distribution. This results in a straightforward estimation of $P(\varepsilon,h|m,n)$, that means a drastic simplification of the process and potentially more accurate estimation of soil physical properties.

Results of this method, applied over the Netherlands, are shown in Figs. 2 and 3. Note that at this period of the year (February), the low or non-existent vegetation layer does not affect significantly the retrieval of soil parameters over agricultural areas (crops and pastures).

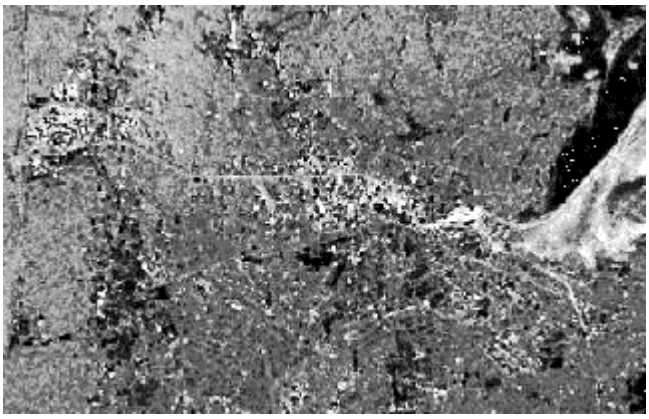

Figure 2: The Netherlands; Feb. 13, 1996. Area size: 38.5x24.5 km. Soil moisture map (ERS/RADARSAT fusion).

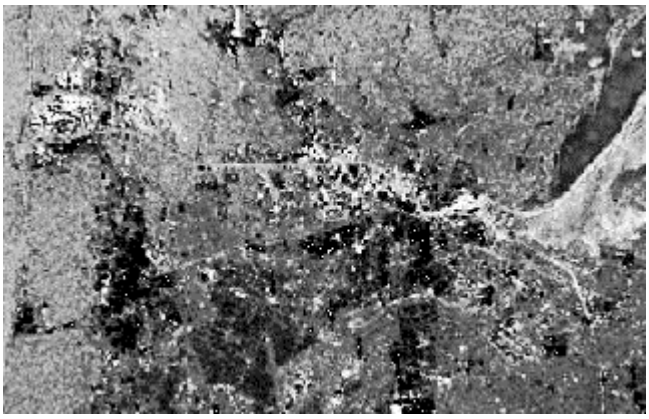

Figure 3: The Netherlands; Feb. 13, 1996. Soil roughness map (inversed LUT), using ERS/RADARSAT data fusion.

In addition, as shown in Fig. 4, snow covered areas (thin snow layer of a few centimeters), difficult to identify in the original SAR images, can easily be identified by simple classification of the soil moisture and roughness maps.

The interest of the quantitative results (especially soil moisture) for the initialisation of agro-meteorological and crop growth models has already been widely expressed. In addition, since soil roughness (in red) allows also the identification of cultivated areas, such a result can be a useful photo-interpretation tool to support other agriculture applications such as early crop surfaces estimation [12], or to monitor special environmental conditions (snow cover, frozen lakes, etc.).

9. CONCLUSION

Two new Bayesian speckle filters have been developed for the pre-processing of multi-channel SAR images, with very convincing results. The Gaussian-Gaussian MAP filter for multi-channel detected multilook SAR images is suitable to process series of images either originating from the same SAR system operating in repeat-pass mode, or from diverse SAR's systems with relatively close properties (in terms of frequency, angle of incidence, spatial resolution and sampling, geometry of images). On the other hand, the Gamma-Gaussian MAP filter for multi-channel detected SAR images is suitable to process

series of images originating from different SAR systems (different frequencies, incidence angles, or spatial resolution for example, but same spatial sampling).
This technique, with special mention to the Gaussian-Gaussian MAP, is able to produce filtered images without loss in spatial resolution. Used in combination with the two-points statistics based algorithm presented in [6], these technique enables even to better restore scene texture and to improve the spatial resolution on point targets. Within homogeneous (textureless) areas, the

Figure 4: The Netherlands on February 13, 1996. Area size: 75.5x52.5 km. Red: soil roughness map. Green: soil moisture map. Blue: snow cover map. Maps produced using ERS-1 and RADARSAT SAR imagery.

efficiency of speckle filtering enables the accurate estimation of σ° required by most remote sensing SAR applications such as the retrieval of soil physical parameters.
In the case of multi-SAR's image series, the speckle filtering process proceeds as a data fusion process, since the information content of the whole image series is exploited to restore all the individual images. Among other advantages, this allows a better detection and restoration of thin scene details.
The extension of this Bayesian filtering technique to the case of a SAR and optical images set is straightforward, as mentioned in Section 3. It is also noticeable that, extending this method to the case of complex SAR images, this technique presents a very interesting potential for super-resolution. The methodology already exists: see [2], for example.
The major interest of this technique is that we apply pure control systems. This offers wide possibilities for the choice and the design of additional commands (statistical and/or physical models) for further data exploitation. In this view, speckle filtering should be regarded as the first step of integrated application oriented control systems rather than of processing chains.

ACKNOWLEDGMENT

The ERS-2 image has been provided by the European Space Agency to PRIVATEERS in the framework of the ERS Pilot Project PE-FRNE2. The RADARSAT image has been provided by the Canadian Space Agency and Radarsat International to PRIVATEERS in the framework of the RADARSAT Pilot Project ADRO#581.

REFERENCES

[1] A. Lopes, E. Nezry, R. Touzi, H. Laur, 1993: "Structure detection and statistical adaptive speckle filtering in SAR images", *Int. J. Rem. Sens.*, Vol.14, n°9, pp.1735-1758.

[2] S.P. Luttrell, 1991: "The theory of super-resolution of coherent SAR images: a review", *Int. J. Rem. Sens.*, Vol.12, n°2, pp.303-314.

[3] E. Nezry, F. Zagolski, A. Lopes, F. Yakam-Simen, 1996: "Bayesian filtering of multi-channel SAR images for detection of thin structures and data fusion", *Proc. of SPIE*, Vol.2958, pp.130-139.

[4] J.S. Lee, 1980: "Digital image enhancement and noise filtering by use of local statistics", *IEEE Trans. on PAMI*, Vol.PAMI-2, n°3, pp.165-168.

[5] R. Touzi, A. Lopes, P. Bousquet, 1988: "A statistical and geometrical edge detector for SAR images", *IEEE Trans. on Geosc. and Rem. Sens.*, Vol.GRS-26, n°6, pp.764-773.

[6] E. Nezry, M. Leysen, G. De Grandi, 1995: "Speckle and scene spatial statistical estimators for SAR image filtering and texture analysis: some applications to agriculture, forestry, and point targets detection", *Proc. of SPIE*, Vol.2584, pp.110-120.

[7] O.D. Faugeras, W.K. Pratt, 1980: "Decorrelation methods of texture feature extraction", *IEEE Trans. on PAMI*, Vol.PAMI-2, n°4, pp.323-332.

[8] Z.S. Haddad, P.C. Dubois, 1994: "Bayesian estimation of soil parameters from remote sensing data", *Proc. of IGARSS'94*, Vol.3, pp.1421-1423, Pasadena, 8-12 Aug. 1994.

[9] M.S. Dawson, A.K. Fung, M.T. Manry, 1995: "Tools for soil moisture retrieval from radar measurements", *Retrieval from bio- and geophysical parameters from SAR data for land applications*, pp.295-305, Toulouse, 10-13 Oct. 1995.

[10] P.C. Dubois, J. van Zyl, T. Engman, 1995: "Measuring soil moisture with imaging radars", *IEEE Trans. on Geosc. and Rem. Sens.*, Vol.33, n°4, pp.915-926.

[11] M. Hallikainen, F.T. Ulaby, M.C. Dobson, M.A. El-Rayes, L. Wu, 1995: "Microwave dielectric behaviour of wet soil - Part 1: Empirical models and experiment observations", *IEEE Trans. on Geosc. on Rem. Sens.*, Vol.GE-23, n°1, pp.25-34.

[12] E. Nezry, G. Genovese, G. Solaas, S. Rémondière, 1995: "ERS based early estimation of crop areas in Europe during the winter 1994/1995", *Proc. of the 2nd ERS Applications Workshop*, ESA SP-383, pp.13-20, 6-8 Dec. 1995.